GEOPHYSICS, VOL. 34, NO. 5 (OCTOBER 1969) P. 739–752, 13 FIGS.

SIMULATION OF TIME-DOMAIN, AIRBORNE, ELECTROMAGNETIC SYSTEM RESPONSE†

A. BECKER*

The response of a time-domain electromagnetic system over a thin conducting sheet may be simulated by purely electronic means and without recourse to scale model experiments. The simulation is based on the similarity between the frequency domain response function for a thin sheet and the transfer function of certain RC active networks. Since this type of experiment employs actual field equipment, the proposed technique also constitutes a valid means of data quality control.

It is difficult to carry out an analog simulation for conductors which do not resemble a thin sheet. If, however, the frequency domain response function for the situation in question is known, the simulation may be carried out on a digital computer. The digital simulation process involves a numerical Fourier decomposition of the primary field waveform (as seen by the receiver), the calculation of the effect of the ground on each harmonic component, and the recombination of the secondary field harmonics to form the observed transient. The technique is illustrated with some calculations of theoretical responses for an EM system over a homogeneous ground and over a thin horizontal conducting sheet. The digital simulation technique is more useful than the analog.

INTRODUCTION

Time-domain airborne EM prospecting has been successfully employed for massive sulfide detection since about 1962 (Barringer, 1962; Boniwell, 1967). More recently, the very same technique has proven to be very useful for the mapping of surficial deposits (Collett, 1965; Baudoin et al, 1967). Inevitably, each successful survey, while indicating new possible applications of this method, also underlined the necessity for further technical and theoretical development. In particular, the Winkler aquifer test (Collett, 1965) executed by the Geological Survey of Canada in 1965 pointed out the need for increased resolution in the data, for airborne magnetic tape recording, for a controlled assessment for equipment performance, and finally for a set of theoretical curves which could be used as an aid to the quantitative interpretation of the flight records. At the request of the Geological Survey of Canada, the manufacturer and inventor of the equipment, Barringer Research Limited, implemented the first two of these requirements. The other two developments were undertaken by the Survey and form the subject of this paper.

System performance can be readily appraised by subjecting the actual system receiver to a series of operational tests. The effect of the various receiver parameters such as bandwidth and center frequency can be thus established. At the same time, the linearity, fidelity, and calibration of the associated electronic circuits are verified.

There are a number of ways in which such tests can be carried out. The first and perhaps the most obvious incorporates a series of carefully controlled test flights. The relative cost of this type of experiment, however, virtually relegates it to the "last resort" category. Classical scale model experiments constitute another solution to this problem. Unfortunately, this technique is rather

† Presented at the 38th Annual International SEG Meeting Denver, Colorado, October 2, 1968. Manuscript received by the Editor October 18, 1968; revised manuscript received March 17, 1969.

* Geological Survey of Canada, Ottawa, Ontario.

difficult to apply in real-time if proper scaling conditions are to be maintained.

The method of analog simulation presented in this paper is relatively free from these defects. It employs the actual field equipment in real-time. Difficulties in scaling are completely eliminated by simulating the conductor-system interaction with the aid of an electronic network.

The method for the creation of master curves is also guided by the principles of simulation. This approach permits the establishment of a set of general computer programs which yield the time-domain response of any particular EM system to a variety of conductor configurations. The main program, which simulates the system behavior, receives all of its input in the frequency domain. It thus becomes possible to incorporate directly the vast amount of frequency domain results currently available (Ward, 1967; Frischknecht, 1967). Equally important is the fact that the effect of any specific system parameter such as receiver response or primary field waveform can be introduced into the main program as readily as in the case of the analog method.

Since the need for the material presented here was mainly derived from our own experience with the Barringer Input[1] system, it is normal that this system would serve as a basis for all further discussion. Similar work has been done on the same system by Nelson and Morris (1969) and by Morrison et al (1969). It is hoped, however, that all the general aspects of the simulation techniques developed in this article will prove applicable to a number of other time-domain EM systems.

SYSTEM RESPONSE SIMULATION—ANALOG METHOD

The analog simulation method is based directly on the operating principles of an EM system (Figure 1). The system is characterized by a transmitter emitting a repetitive primary field which is specified by its discrete frequency spec-

[1] Registered Trademark of Barringer Research.

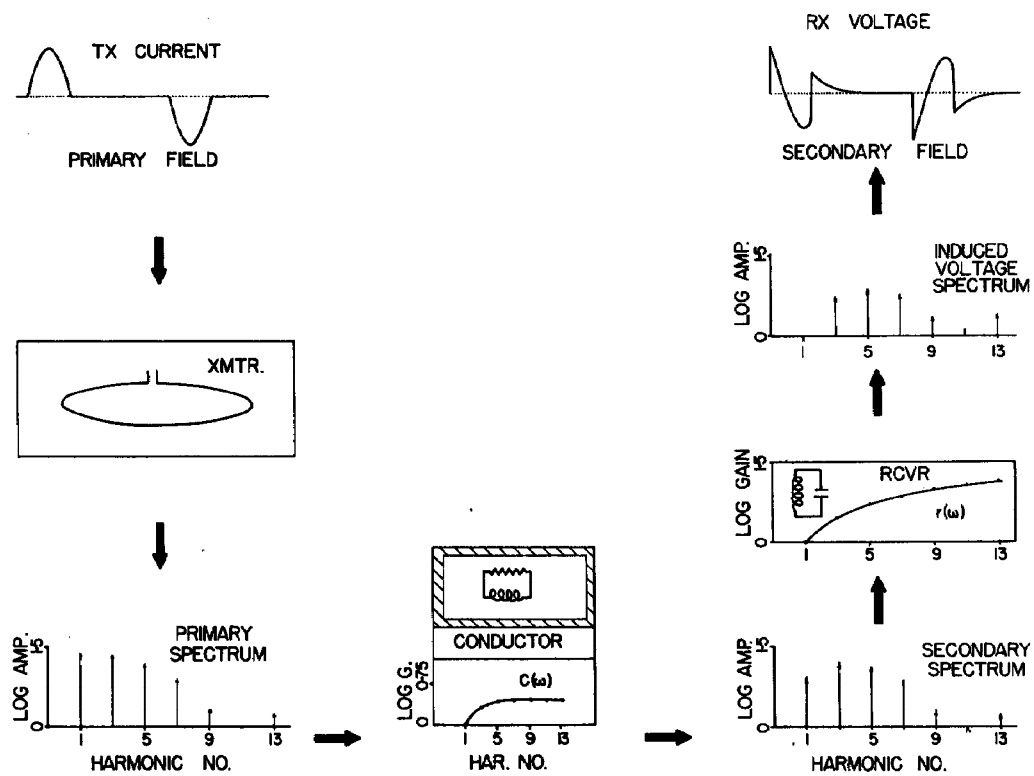

FIG. 1. Pictorial description of electromagnetic induction process.

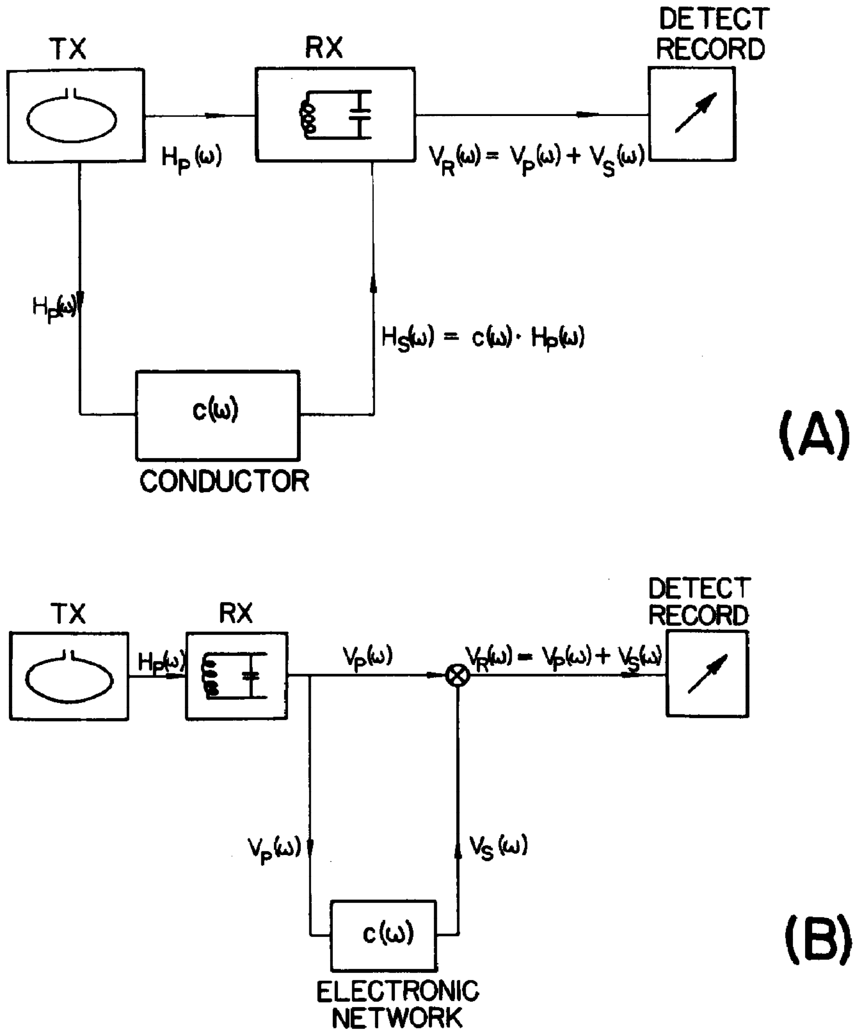

FIG. 2. Physical basis for the analog simulation technique. (A) Schematic diagram for actual system. (B) Schematic diagram for equivalent analog model.

trum $h_p(\omega)$, a conductor described by its frequency dependent transfer function $c(\omega)$, and a receiver which supplies a voltage $V_R(t)$ to the detector. From a spectral point of view, all conductors have a high-pass filtering effect on the primary field. The main effect of the receiver transfer function $r(\omega)$ is a differentiation of the magnetic field. Thus the voltage induced in the receiver by the secondary field resembles a distorted differential of the primary field. Of sole interest to us is the transient which terminates the main waveform. Only this part of the receiver voltage is sampled, detected, and recorded by the receiver electronics (Barringer, 1962; Boniwell, 1967).

Although the EM system under consideration apparently functions in the time domain, the analog simulation method is most easily derived by considering the matter in the frequency domain. Let us examine a block diagram for the total system (Figure 2A). One can conceptually visualize the interaction of the EM system with the conductor as a simple linear filtering process and describe it in terms of conventional electrical engineering terminology. In particular, if one expresses the repetitive primary field waveform $H_p(t)$ in terms of its complex Fourier series,

$$H_p(t) = \sum_{n=-\infty}^{n=+\infty} h_p(n\omega_0)e^{jn\omega_0 t}, \qquad (1)$$

and the voltage output of the receiver in terms of its Fourier series

$$V_R(t) = \sum_{n=-\infty}^{n=+\infty} v_R(n\omega_0)e^{jn\omega_0 t}, \qquad (2)$$

the linear relationship between the two sets of coefficients can be demonstrated. To derive the exact relation it is convenient to define the receiver in terms of its frequency dependent transfer function,

$$r(n\omega_0) = \frac{v(n\omega_0)}{h(n\omega_0)}, \qquad (3)$$

which relates the receiver output voltage coefficients $v(\omega)$ to the inducing field coefficients $h(\omega)$. In a similar manner it is necessary to ascribe to the conductor a frequency dependent transfer function $c(\omega)$ which defines the relation between the secondary and primary field coefficients at the receiver through

$$c(n\omega_0) = h_s(n\omega_0)/h_p(n\omega_0). \qquad (4)$$

The coefficients for the output voltage induced in the receiver by the primary field can now be written as

$$v_p(\omega) = r(\omega)\cdot h_p(\omega); \qquad (5)$$

similarly those induced by the secondary field are given by

$$v_s(\omega) = r(\omega)\cdot h_s(\omega). \qquad (6)$$

With the help of equation (4), relation (6) can be rewritten as

$$v_s(\omega) = r(\omega)\cdot c(\omega)\cdot h_p(\omega), \qquad (7)$$

or

$$v_s(\omega) = c(\omega)\cdot v_p(\omega). \qquad (8)$$

The sum of the coefficients for voltage output of the receiver is of course given by the sum of the primary and secondary coefficients,

$$v_R(\omega) = v_p(\omega) + v_s(\omega)$$

which, upon substitution of equation (8) can be written as

$$v_R(\omega) = v_p(\omega)\cdot[1 + c(\omega)]. \qquad (9)$$

This establishes the linear relation between the receiver output and the primary field coefficients.

The theoretical foundation of the analog simulation method now becomes apparent. In fact equation (9) linearly relates the receiver output voltage harmonic coefficients when a conductor is present $[c(\omega)\neq 0]$ to the harmonic coefficients of the receiver output in the absence of any conducting material $[v_p(\omega)]$. To simulate a conductor with a transfer function $c(\omega)$, it is only necessary to insert between the receiver and the detector a linear filter network whose transfer function is also $c(\omega)$, and to add the output of the network to the "free space" output of the receiver. Figure 2B illustrates the schematic arrangement of the equipment. The analogy between the two illustrations of Figure 2 is complete since the mathematical expressions which govern the voltage applied to the detecting mechanism [(2) and (9)] are common and identical in both cases.

The electronic analog system consists of a scaled down model of the aircraft transmitter and its receiver, arranged in a maximum coupled configuration. The scaling factor is of no consequence. It is most important, however, that the excitation current in the transmitter be nearly identical in waveform and repetition rate to that used in practice, and that the band-pass characteristics of the laboratory receiver closely resemble those of the actual pick-up coil-amplifier assembly. The conductor is replaced by an electronic network with a transfer characteristic approximately equal to that of the conductor whose response is being simulated. The network is excited with the voltage induced in the receiver by the primary magnetic field. Its output should be multiplied by a constant which depends on the transmitter-conductor-receiver geometry. If a full simulation is desired, a portion of the receiver voltage (depending on the XMTR-RCVR configuration) should be added directly to the network output. In practice, one is mainly concerned with the detector response to the secondary field transient which terminates the received waveform, and the above step may be omitted.

The artificially generated transient can now serve as a basis for the quality assessment of the detection apparatus. If the experimental set-up is closely controlled, the transients generated by it can be made identical to those which would be observed by flying the detector over different conducting masses. Since the detector employed in the laboratory is the very same piece of equipment that is used on survey, use of this method results in a laboratory study of the equipment response under quasi-operational conditions.

Perhaps the simplest test to perform is the evaluation of the system's response to a small ring of conducting material. Although this type of body does not occur in nature, its electromagnetic characteristics sufficiently resemble those of naturally occurring conductors to warrant its consideration. The utilization of this rather simple conductor carries with it two important advantages. First, transients generated by this type of anomaly decay with time in a truly exponential manner (Grant and West, 1965, p. 540–543), and thus provide an immediate check on detector fidelity. The main advantage, however, is derived from the fact that its transfer function is a simple algebraic expression which readily lends itself to simulation.

The transfer function for a ring conductor (Figure 3) is given by,

$$c(\omega) = (\text{G.F.}) \frac{\alpha^2 + j\alpha}{1 + \alpha^2} \tag{10}$$

(Grant and West, 1965, p. 488). Here, the term (G.F.) denotes a geometrical factor which is a function of spatial relations between the transmitter, the receiver, and the conductor. The frequency-dependent, dimensionless, induction parameter α is related to the ring's time constant τ through

$$\alpha = \omega\tau = \omega L/R, \tag{11}$$

where L is the ring inductance, R its resistance, and ω is the angular frequency. All units are in the mks system.

On the other hand, if we consider the electronic network also shown in Figure 3, we note that its transfer function is given by

$$c'(\omega) = [\text{G.F.}] \frac{R}{R + \dfrac{1}{j\omega c}} \tag{12}$$

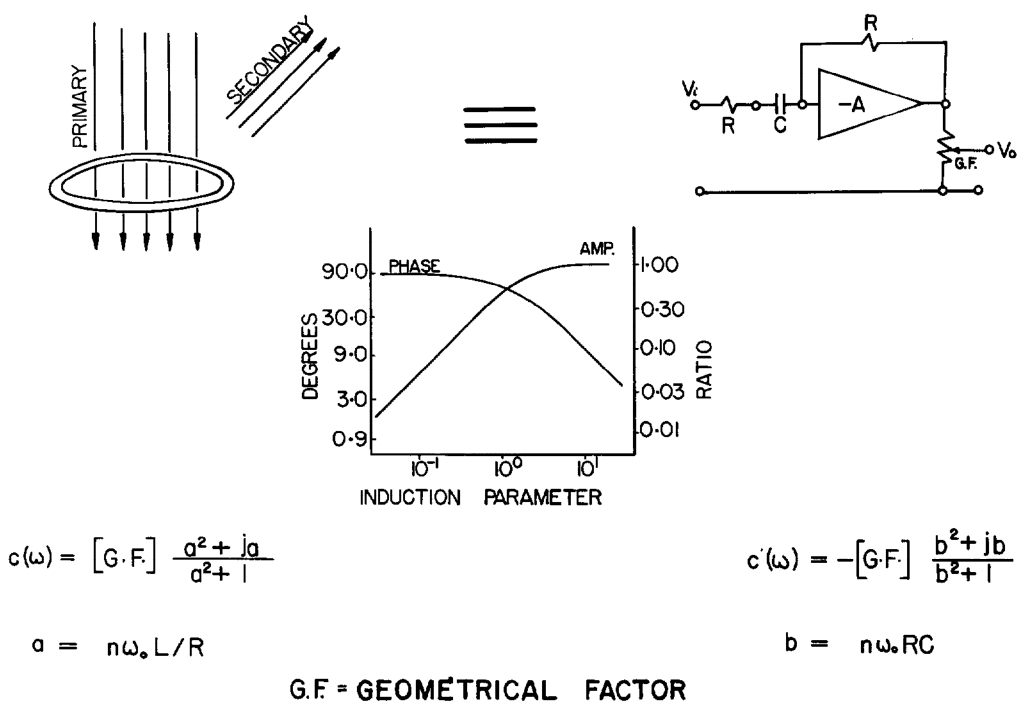

FIG. 3. Equivalence of electronic and electromagnetic transfer functions.

(Karplus, 1958, p. 233), where R is the resistance of both the feedback and series resistors, and C is the series capacitance. The [G.F.] term denotes the fraction of the output voltage made externally available. With some minor algebra, expression (12) can be put into a form identical to equation (10), i.e.,

$$c'(\omega) = -[\text{G.F.}](\beta^2 + j\beta)/(1 + \beta^2). \quad (13)$$

In this case,

$$\beta = \omega cR = \omega\tau', \quad (14)$$

where τ' is the time constant of the network. In order to employ the network for simulation it is only necessary to have,

$$c(\omega) = c'(\omega)$$

for all frequencies. This can be readily accomplished by making

$$(\text{G.F.})_{\text{network}} = (\text{G.F.})_{\text{conductor}},$$

and

$$\tau' = \tau.$$

In terms of the actual electrical parameters we must have

$$(L/R)_{\text{conductor}} = (CR)_{\text{network}}. \quad (15)$$

The difference in sign between the two transfer functions will result in a difference in sign between the theoretical and simulated transients. Their magnitude and shape, however, will be identical. Should this present any difficulty, it may be remedied by adding to the simulation network a unit gain inverting stage.

Figure 4 illustrates the results obtained in a series of tests on the receiver from the EM system under consideration. It can readily be appreciated that the fidelity of the piece of equipment under test was entirely satisfactory over a variety of time constants. It was also demonstrated that the calibration of the detector was correct because the differences between the experimental and theoretical data (obtained by the digital simulation method) did not exceed the noise level of the instrument.

It is perhaps somewhat fortuitous that the response of a thin, conducting sheet may, under certain conditions, also be simulated with the aid of the simple RC network just discussed.

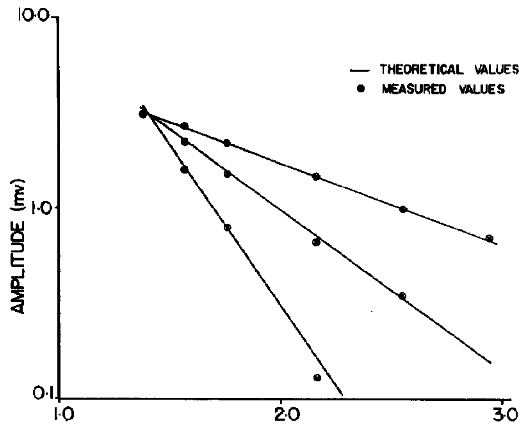

FIG. 4. Fidelity test on receiver from the system under discussion by comparison of measured and theoretical data for various time constants.

The analogy is derived empirically by observing that the response of the sheet to an EM airborne system whose flight elevation is of the order of its coil separation is similar to the response function of a ring conductor (Frischknecht, 1967). The theoretical basis for the sheet ring analogy consists of the fact that at high frequencies the sheet behaves as a plane mirror which images the transmitter at a depth below the conducting sheet equal to the transmitter's height above it. In particular, at high frequencies the transfer function for the network, $c_n(\omega)$, may be written as

$$c_n(\omega) = [\text{G.F.}](1 + j/\beta), \quad (16)$$

while the transfer function for the thin sheet at high frequency is given by (Wait, 1953) as

$$c_s(\omega) = [\text{G.F.}](1 + \kappa j/\gamma), \quad (17)$$

where

$\gamma = \mu\omega\sigma t_s/2$,
μ = sheet permeability,
σ = sheet conductivity,
t = sheet thickness,
s = transmitter-receiver horizontal separation,
$\kappa \equiv$ a geometrical constant, which is a function transmitter-receiver geometry and flight elevation, and
all units are in the mks system.

It is now evident that high-frequency equality of the two transfer functions may readily be established by choosing,

$$\beta = \gamma/\kappa,$$

which is equivalent to choosing the network time-constant

$$\tau_{\text{network}} = \mu\sigma t s/2\kappa. \qquad (18)$$

It is of course also necessary to allow directly for the effect of aircraft elevation and receiver-transmitter geometry by controlling the gain of the electronic network. A typical set of results is shown in Figure 5. These results were obtained for a coplanar vertical axis system flown at 345 ft with a coil separation of 360 ft. The appropriate value of κ was equal to unity. Network time constants were set equal to 0.25, 0.5, and 1.0 ms, corresponding to sheet thickness-conductivity product values of 3.6, 7.2, and 14.5 mhos, respectively. The theoretical values used for comparison were obtained with the method discussed in the next part of this paper.

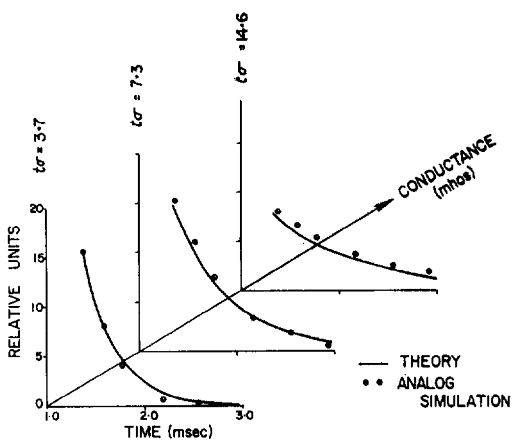

FIG. 5. Results for analog simulation of thin sheet response.

SYSTEM RESPONSE SIMULATION—DIGITAL METHOD

The digital computer programs for the evaluation of theoretical response curves were generated through a purely operational approach. The simulative aspect of these programs is derived from the provisions, incorporated within the general framework, for the description of a variety of features particular to different airborne installations. In this manner, the effects of transmitter waveform, receiver bandwidth and damping, and detector channel widths and settings may be fully introduced in the computation of master curves. The principal feature of this technique, however, is the direct translation of theoretical or scale-model frequency domain data into time-domain response curves.

The digital simulation method is based on the same principles that were used for the derivation of the analog method (Figure 6). The starting point is the evaluation of the Fourier coefficients for the voltage induced in the receiver by the primary magnetic field $V_p(t)$. If we write

$$V_p(t) = \sum_{n=-N}^{n=N} v_p(n\omega_0)e^{jn\omega_0 t}, \qquad (19)$$

it is possible to evaluate the N complex coefficients V_p with the help of standard numerical methods (Hamming, 1962, p. 67-74). The accuracy of the expansion of course depends on the number of coefficients computed. For our purposes, it was found that satisfactory accuracy was obtainable with the use of 352 harmonics. Since the EM system under discussion utilizes a mirror-symmetrical (Goldman, 1948, p. 9) excitation function the even harmonic coefficients are zero and only odd harmonics need be considered.

The next step in the digital simulation is the evolution of the Fourier coefficients, $v_s(n\omega_0)$, of the voltage induced in the receiver by the secondary field. These can be written directly from equation (8) as

$$v_s(n\omega_0) = c(n\omega_0)\cdot v_p(n\omega_0). \qquad (20)$$

Here the $c(n\omega_0)$ are the complex, frequency domain, transfer function values for the system and conductor in question. Normally, these are not available in closed analytical form and must be obtained by interpolation in a table of values such as the one given by Frischknecht (1967).

At this point, one can compute the time-domain values of the voltage induced in the receiver by the secondary field through a summation of the corresponding finite Fourier series

$$V_s(t) = \sum_{n=-N}^{n=N} v_s(n\omega_0)e^{jn\omega_0 t}. \qquad (21)$$

In practice, however, the detector employed does not yield $V_s(t)$ but, because of finite sampling channel widths, measures the average value of this quantity

$$\overline{V_s(t)} = \frac{1}{2\Delta}\int_{t-\Delta}^{t+\Delta} V_s(t)dt, \qquad (22)$$

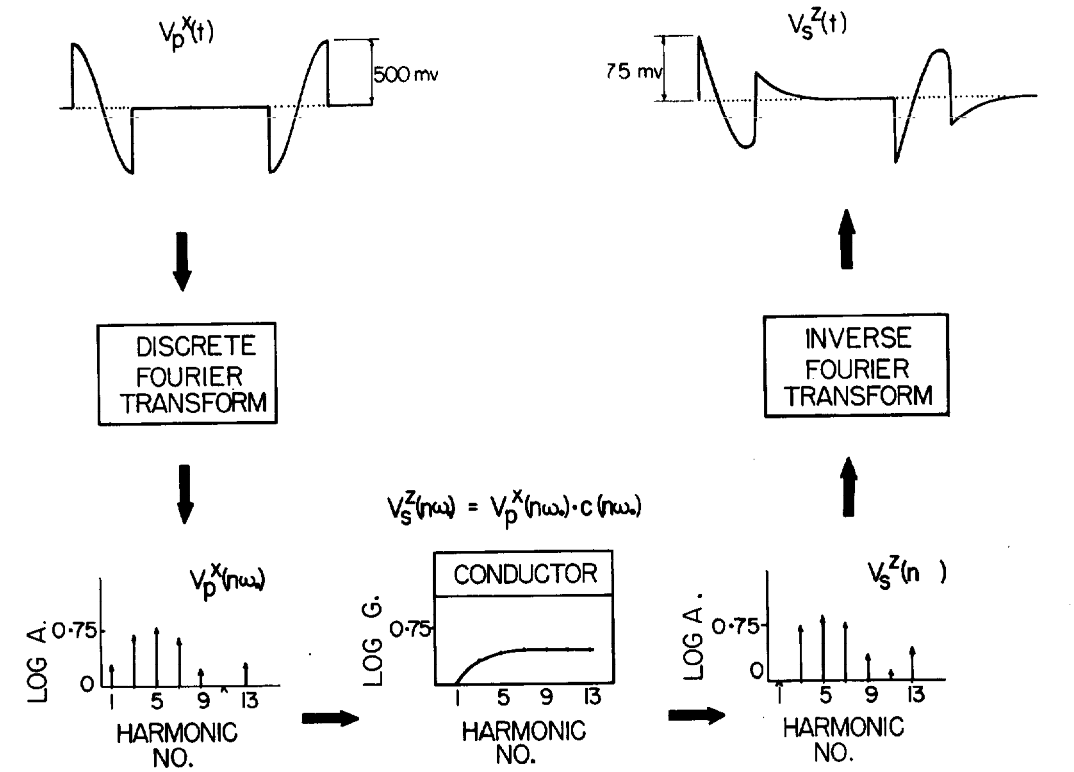

FIG. 6. Block diagram for digital simulation method.

where 2Δ is the sampling channel width. Since $V_s(t)$ is a periodic function, $\overline{V_s(t)}$ will also be periodic. It may then be represented by a Fourier expansion

$$\overline{V_s(t)} = \sum_{n=-N}^{n=N} \bar{v}_s(n\omega_0)e^{jn\omega_0 t}. \tag{23}$$

The coefficients for the Fourier expansion of $\overline{V_s(t)}$ are then simply related to those for the expansion of $V_s(t)$ (Hamming, 1962, p. 298) through

$$\bar{v}_s(n\omega_0 t) = [v_s(n\omega_0)]\cdot[\sin\theta/\theta] \tag{24}$$

with $\theta = n\omega_0\Delta$.

The exact waveform of the voltage induced in the receiver by the horizontal component of the primary field which initiates the computation of the secondary field transients is of great importance. It evidently has a direct bearing on the amplitudes and, to a lesser degree, on the shape of the computed decay curve. In fact, this fundamental quantity contains all the necessary information about the transmitted current wave-

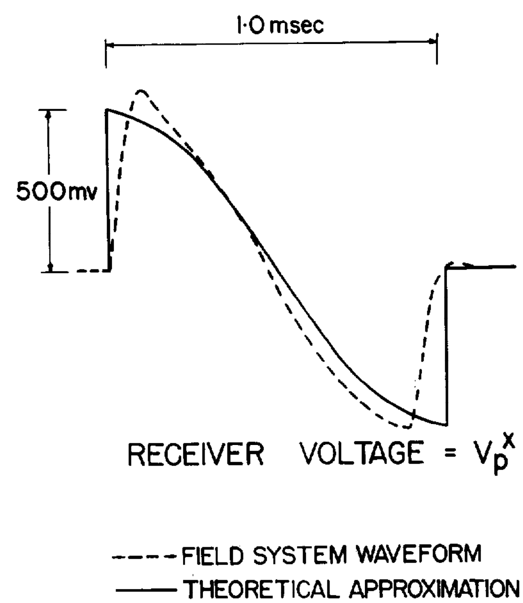

FIG. 7. Theoretical and experimental waveforms for the voltage induced in the receiver by the primary field.

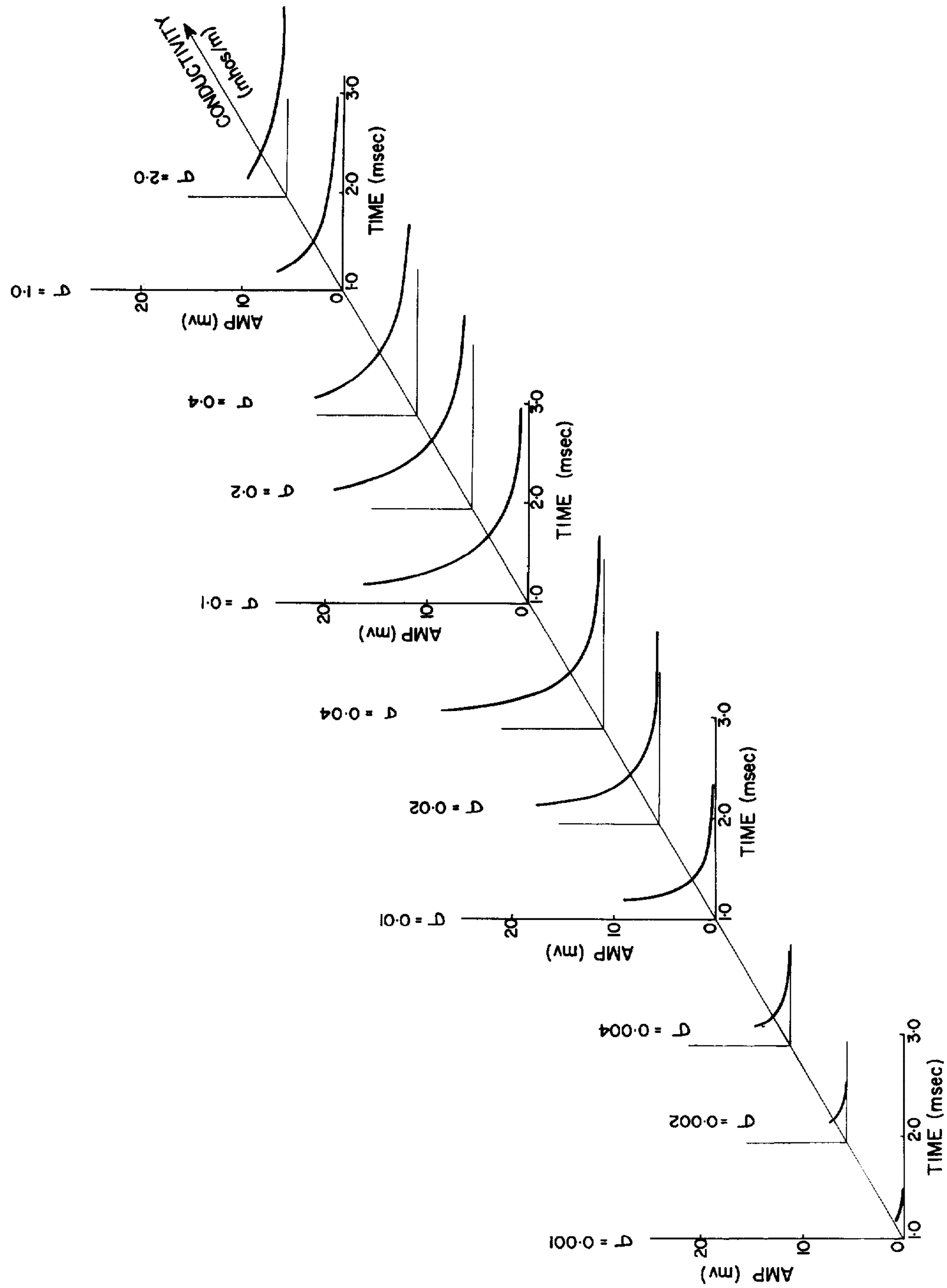

FIG. 8. System response—homogeneous ground.

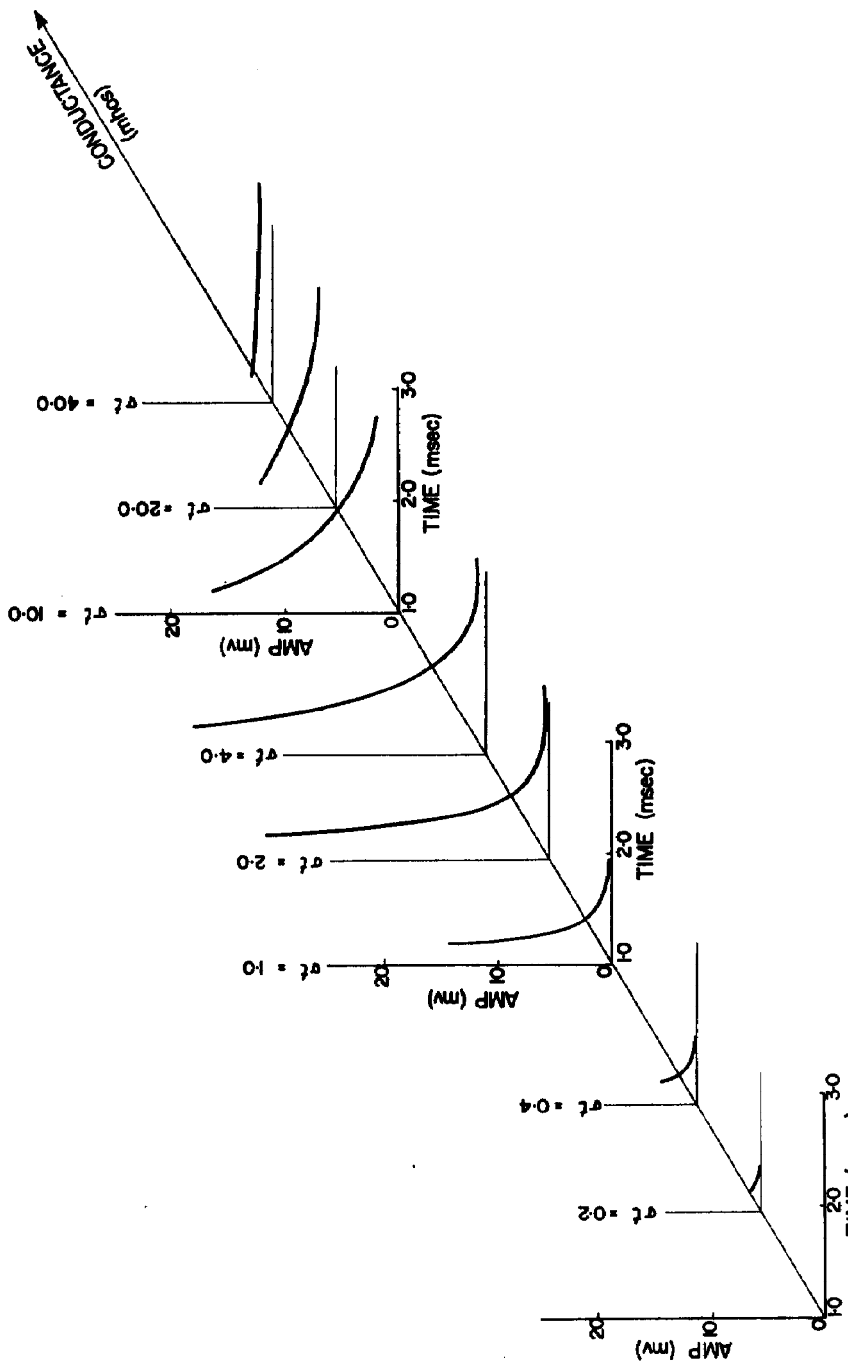

FIG. 9. System response—thin conducting sheet.

form, the electronic parameters of the receiver, and its associated cable amplifier and pre-amplifier gains. The measurement or calculation of the primary waveform thus constitutes an effective calibration of the total system. In practice a direct measurement is preferred to calculation based on the engineering specifications of the system. The experimental calibration may be carried out during the course of a single high altitude test flight. The aircraft should be flown at an elevation in excess of 2500 ft if the effects of ground conductivity are to be made negligible.

The digital computer program ensemble included programs for Fourier analysis and Fourier synthesis, and was complemented with table look-up and Newton interpolation subroutines. With the incorporation of the 176 odd harmonic components we were able to achieve an accuracy of about one-twentieth of one percent of the peak amplitude of the primary field. The frequencies considered ranged from the fundamental at 144 Hz to the last harmonic at about 50 kHz. Once the programs are loaded, the computer takes about 25 sec to produce a set of transient decay values. The running cost per master curve thus amounts to just over one dollar.

DIGITAL SIMULATION—RESULTS

The following results were computed for an analytical half-cosine excitation function (Figure 7). While the chosen function only approximates the primary induced voltage which might be observed in a practical case, we have elected to employ this general theoretical function rather than any particular experimental waveform to serve as a basis for subsequent discussion. Evidently, the preparation of master curves for any particular system should be based on its own primary field response. With one exception all the curves presented here describe the terminal secondary field transients for a minimum coupled airborne system with vertical transmitter and receiver axes. The receiver is situated 360 ft behind and 260 ft below the aircraft. Flight elevation was taken

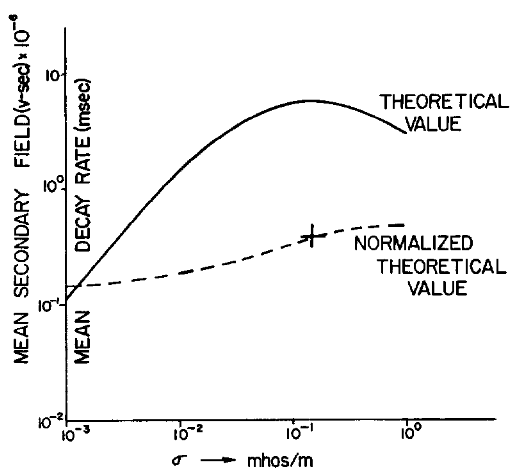

Fig. 10. Relation of mean transient amplitudes (area under decay curve) and mean decay rates to conductivity of half space.

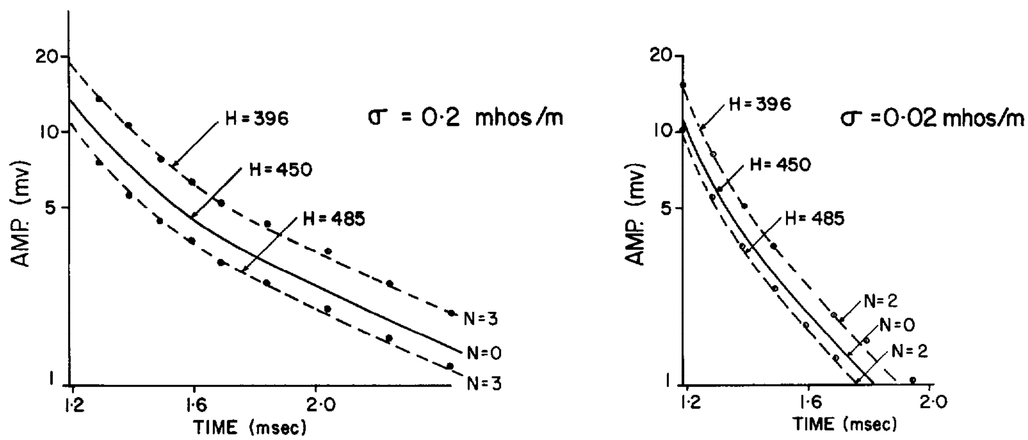

$$A = A(H_0)\cdot(H/H_0)^{-N}$$

Fig. 11. Variation of transient amplitude with elevation.

to be 450 ft. Again with one exception, all times indicated are taken with reference to the onset of the primary field pulse.

The first study undertaken with the aid of the digital simulation program ensemble examined the response of a homogeneous half-space (Figure 8). The system under consideration responds well to ground resistivity values which range from 100 to 2 ohm-m. Outside of this range, however, transient amplitudes fall sharply. A close investigation of the transient shape reveals that the amplitude decay with time nearly follows an inverse power law. The negative exponent appears to be uniformly related to the ground resistivity.

It is interesting to compare the homogeneous ground transients with those that would be obtained over a thin horizontal sheet (Figure 9). Sizable responses in this case are limited to sheet conductance values (conductivity—thickness product) which range upward from 0.5 to 20 mhos. Within this range transient, amplitudes may be up to fifty percent larger than those produced by the homogeneous ground. With the exception of the fact that thin sheet transients decay in an almost exponential mode, it is rather difficult to distinguish these from a homogeneous ground response.

It is possible to summarize the transient variation with ground conductivity by computing the area under the total decay curve. This quantity (Figure 10) which is proportional to the mean transient amplitude has been found quite useful (Collett, 1967) in the preliminary evaluation of airborne, time-domain, EM data. Unfortunately the loss in mean transient amplitude with conductivity which occurs above a value of about 0.1 mho/m restricts the use of this technique to low conductivity values. The difficulty may be re-

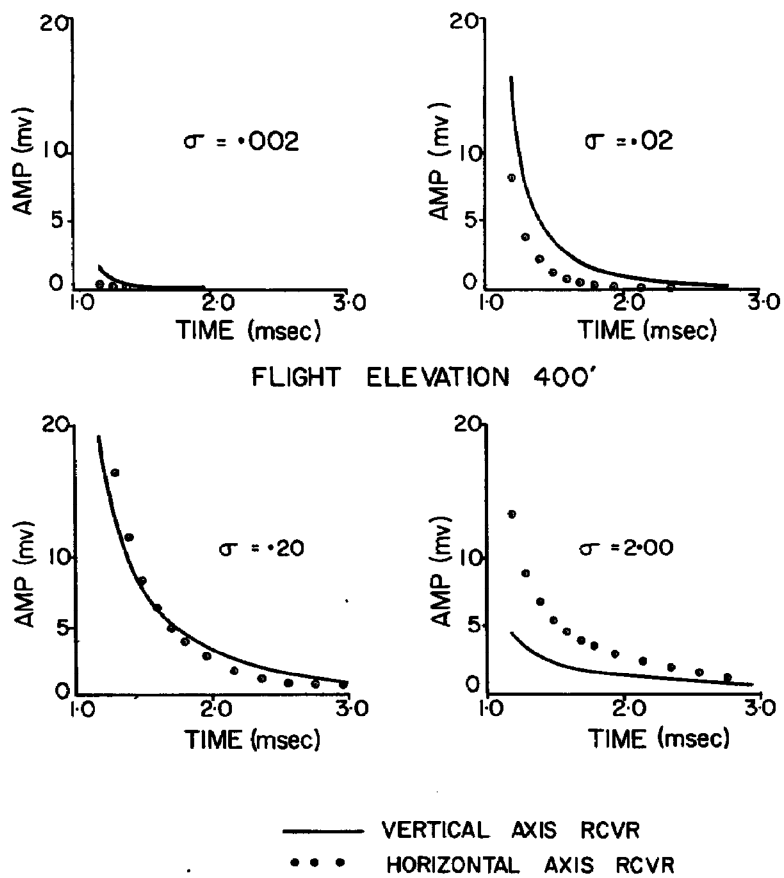

FIG. 12. Variation of transient amplitude with receiver axis orientation.

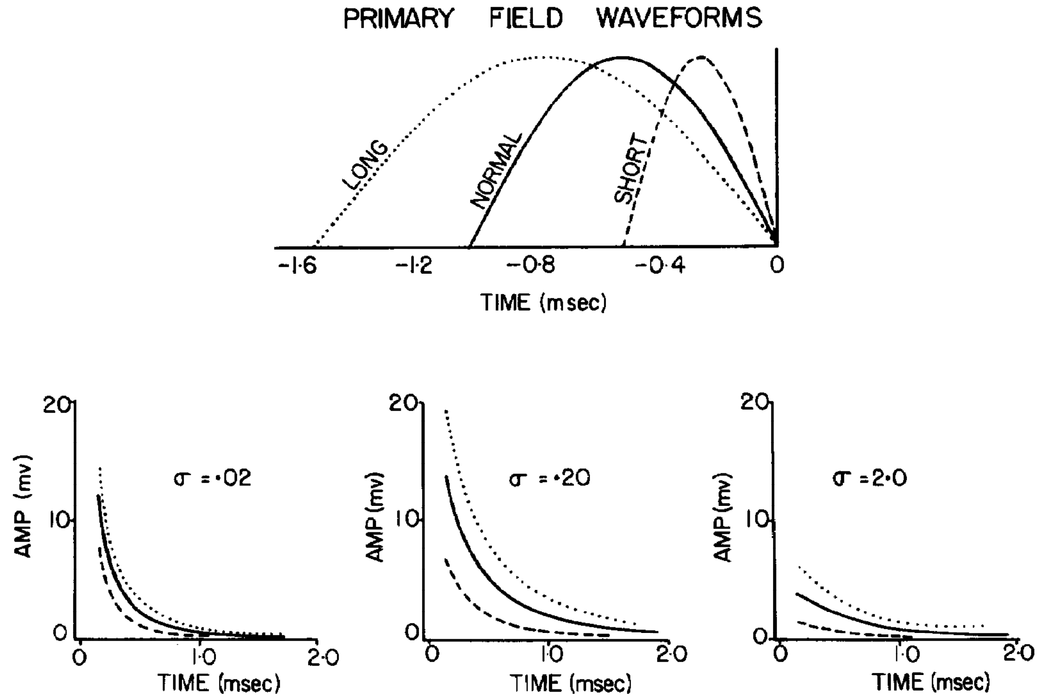

FIG. 13. Variation of transient amplitude with primary field duration.

solved by normalizing the "area under the curve" function with respect to the initial (Channel 1) transient amplitudes. The resulting normalized theoretical curve is closely related to the average decay rate and provides the necessary information for an unique determination of ground conductivity.

In addition to the compilation of standard response curves we have taken advantage of the digital method to examine the variation of transient behavior with changing survey conditions. These mathematical experiments permitted us to investigate the effects of transmitter-receiver-conductor geometry and the effects of the instrument electronic parameters on the theoretical values of the secondary field decay curve.

For example, an initial investigation of transient amplitude variation with flight elevation (Figure 11) indicates this to be a rather complex matter as the rate of transient amplitude fall-off with elevation appears to be a function of the ground conductivity. It seems that over conductive ground (5 ohm-m), the transient amplitude varies inversely as the cube of the elevation, while over a moderately resistive terrain it decreases much less rapidly, following an inverse square law. The transient shape, however, appears to remain unaltered with the small elevation changes considered here.

Another set of computations was devoted to a comparison between the results obtainable with the receiver axis horizontal and those which would be obtained with a vertical receiver axis (Figure 12). It can be readily appreciated that in the absence of anomalously high conductivities a vertical receiver axis is to be preferred when the system is used for geological mapping.

The last set of calculations which we wish to present here demonstrates the desirability of employing long primary current pulses (Figure 13). As may have been expected (Bhattacharyya, 1968), the resultant transient amplitudes vary uniformly with primary pulse duration.

SUMMARY AND CONCLUSIONS

The methods and ideas presented in this paper may appear to be somewhat idealized since their application was illustrated only with respect to some very simple conductor configurations. The conductor configurations for which system response was determined were not chosen however with the accent on the specific results. The main purpose of the examples was to illustrate the flexibility of the proposed techniques.

By virtue of its simplicity, the analog method provides a rapid and effective means for assessing the response of a given time-domain system to some simple conductor configurations. Most conductors, however, cannot be simulated with elementary electronic networks. The usefulness of this technique thus remains momentarily restricted to equipment tests during development and to the large measure of data quality control which it can provide.

The digital-simulation technique is much more useful. It may be used to compute the system response to any set of conditions for which frequency domain data is available. In this paper we have only examined the effects of ground conductivity, receiver-transmitter coupling, and primary field waveform. The very same method, however, can also be used to study, for example, the effects of receiver band width and to simulate the secondary field transients which are generated by spherical, cylindrical, and thin sheet conductors.

It is sincerely hoped that the digital technique presented here may be soon developed to the point where it will prove useful for the automatic digital computer interpretation of the field results. The vast amount of available survey data certainly warrants the pursuit of this goal!

ACKNOWLEDGMENTS

It is a pleasure to acknowledge with thanks the use of the EM equipment supplied gratuitously by Barringer Research Ltd. for the laboratory tests.

REFERENCES

Barringer, A. R., 1962, The INPUT electrical pulse prospecting system: Min. Cong. J., v. 48, p. 49–52.
Baudoin, P., Durozoy, G., Utard, M., 1967, Etude par prospection electromagnetique aerienne (Methode INPUT) d'un contact eau douce—eau sales dans le delta du Rhone: Presented at the Canadian Centennial Geophysical Conference, Niagara Falls.
Bhattacharyya, B. K., 1968: Personal communication.
Boniwell, J. B., 1967, Some recent results with the INPUT airborne EM system: CIMM Bull., v. 60, p. 325–332.
Collett, L. S., 1965, The measurement of the resistivity of surficial deposits by airborne pulsed electromagnetic equipment: Presented at 35th Annual SEG Meeting, Dallas, Texas.
——— 1967, Personal communication.
Frischknecht, F. C., 1967, Fields about an oscillating magnetic dipole over a two layer earth and application to ground and airborne electromagnetic surveys: Quarterly of the Colorado School of Mines, v. 62, No. 1.
Goldman, S., 1948, Frequency analysis, modulation and noise: Toronto, McGraw-Hill.
Grant, F. S., West, G. F., 1965, Interpretation theory in applied geophysics: Toronto, McGraw-Hill.
Hamming, R. W., 1962, Numerical methods for scientists and engineers: Toronto, McGraw-Hill.
Karplus, W. J., 1958, Analog simulation: Toronto, McGraw-Hill.
Morrison, H. F., Phillips, R. S., and O'Brien, D. P., 1969, Quantitative interpretation of transient electromagnetic over a layered half space: Geophys. Prosp., v. 17, p. 82–101.
Nelson, P. H., and Morris, D. B., 1969, Theoretical response of a time-domain airborne electromagnetic system: Geophysics, v. 34, p. 729–738.
Wait, J. R., 1953, Induction in a conducting sheet by a small current-carrying loop: Appl. Sci. Res., Sec. B, v. 3, p. 230–236.
Ward, S. H., 1967, Electromagnetic theory for geophysical applications, *in* Mining geophysics, V. II, Ch II: Soc. Explor. Geophys., p. 10–372.